

# Fingerprinting CANDO: Increased Accuracy with Structure and Ligand Based Shotgun Drug Repurposing

1 James Schuler and Ram Samudrala\*

*Department of Biomedical Informatics, Jacobs School of Biomedical Sciences at the University at Buffalo, Buffalo, NY*

E-mail: ram@compbio.org

Phone: (716) 888-4858

2 We have upgraded our Computational Analysis of Novel Drug Opportunities (CANDO)  
3 platform for shotgun drug repurposing to include ligand-based, data fusion, and decision tree  
4 pipelines. The first version of CANDO implemented a structure-based pipeline that mod-  
5 eled interactions between compounds and proteins on a large scale, generating compound-  
6 proteome interaction signatures used to infer similarity of drug behavior; the new pipelines  
7 accomplish this by incorporating molecular fingerprints and the Tanimoto coefficient. We  
8 obtain improved benchmarking performance with the new pipelines across all three evalua-  
9 tion metrics used: average indication accuracy, pairwise accuracy, and coverage. The best  
10 performing pipeline achieves an average indication accuracy of 19.0% at the top10 cutoff,  
11 compared to 11.7% for v1, and 2.2% for a random control. Our results demonstrate that the  
12 CANDO drug recovery accuracy is substantially improved by integrating multiple pipelines,  
13 thereby enhancing our ability to generate putative therapeutic repurposing candidates, and  
14 increasing drug discovery efficiency.

## 15 **Introduction**

### 16 **Drug repurposing**

17 Bringing a new drug to the market may cost hundreds of millions of dollars and takes years  
18 of work.<sup>1</sup> Drug repurposing is the process of discovering a new use for an existing drug.<sup>2,3</sup>  
19 This process may take advantage of existing data on safety and pharmacokinetic properties  
20 from previous trials and clinical use to reduce costs and time associated with traditional drug  
21 discovery. Classic examples of drug repurposing include sildenafil (Viagra) and thalidomide,  
22 which initially were developed to treat chest pain and morning sickness, but were repurposed  
23 to treat erectile dysfunction and erythema nodosum leprosum respectively.<sup>2,4,5</sup> Drugs which  
24 have already been repurposed once are being researched for even more novel uses. For exam-  
25 ple, raloxifene was originally indicated for prevention of osteoporosis and was subsequently  
26 approved for risk reduction in the development of breast cancer.<sup>6</sup> More recently, raloxifene  
27 has been suggested as a possible treatment for Ebola virus disease<sup>7-9</sup>. These examples of  
28 putative and/or successful drug repurposing underlies the diverse mechanisms through which  
29 a single compound may treat a variety of disease types.<sup>10,11</sup> High throughput, target-based,  
30 and phenotypic screening of compounds can be used to generate putative candidates for re-  
31 purposing.<sup>12</sup> For example, potential treatments for Zika virus infection were identified using  
32 a phenotypic screen.<sup>13</sup>

### 33 **Computational drug discovery and repurposing**

34 Finding new drugs or new uses for existing drugs computationally takes advantage of the  
35 growing amount of data generated from wet lab experiments accessible on the Internet,  
36 increased computational power, and higher fidelity of computational models to reality. Ap-  
37 proaches to computational drug discovery and repurposing have been classified as structure-  
38 based or ligand-based.<sup>14-16</sup> In structure-based methods, the structure of a target macro-  
39 molecule, usually a protein, is used to identify small compounds that modulate its behavior.

40 The structure may have been determined via x-ray diffraction or Nuclear Magnetic Res-  
41 onance (NMR), or modeled using template-free (*de novo*) or template-based (homology)  
42 modeling.<sup>17–19</sup> Molecular docking and/or rational drug design is then used to identify lig-  
43 ands that specifically fit into a protein groove or active site.<sup>20,21</sup> In ligand-based methods, the  
44 focus is on the compound, and similarity between representations is used to assess whether  
45 a compound modulates the activity of a target or treat a disease like a known drug. Exam-  
46 ples of ligand-based drug design include 2D and 3D similarity searching,<sup>22</sup> pharmacophore  
47 modeling,<sup>23</sup> and quantitative structure activity relationships (QSAR).<sup>14</sup>

48 Data fusion is a technique in the field of cheminformatics for combining intermolecular  
49 similarity data from different sources or methods.<sup>24–26</sup> Compounds are ranked relative to  
50 each other based on the similarity scores. Multiple rankings of compounds produced by  
51 different methods of detecting similarity may be combined into a single ranking.<sup>24</sup> Ideally,  
52 disparate sources or types of data may yield orthogonality or complementarity in results,  
53 i.e., different top compounds are captured and reported as putative therapeutics for different  
54 reasons.<sup>27,28</sup> For example, Tan et al. obtained an increased recall rate in a virtual screening  
55 experiment using ligand-based two dimensional fingerprint data fused with structure-based  
56 molecular docking energies.<sup>29</sup> Ligand- and structure-based methods have been combined  
57 for use in virtual screening pipelines and platforms, with successes reported in the use of  
58 sequential, parallel, and hybrid techniques for data integration.<sup>28</sup> Data fusion has been also  
59 been used to devise weighting schemes for correct dosing.<sup>30</sup>

60 Newer computational techniques for drug discovery and repurposing gaining in promi-  
61 nence go beyond the structure and ligand-based categorization. The Connectivity Map is  
62 a “reference collection of gene-expression profiles from cultured human cells treated with  
63 bioactive small molecules”,<sup>31</sup> i.e., a tool to identify changes in gene expression due to a  
64 compound or a disease. If a compound causes changes in gene expression level opposite to a  
65 disease (for instance, a disease causes up-regulation of the expression of a set of genes, and  
66 the compound causes down-regulation of the same set of genes), then that compound is con-

67 sidered to be therapeutically useful in the treatment of that disease.<sup>31</sup> Peyvandipour et al.  
68 combined an updated version of the Connectivity Map with knowledge of drug-disease gene  
69 networks, measuring the perturbation effect of drugs on whole systems. Using this model,  
70 they predicted novel treatments for idiopathic pulmonary fibrosis, non-small cell lung can-  
71 cer, prostate cancer, and breast cancer, while simultaneously improving the recall rate of  
72 known drug-disease associations.<sup>32</sup> Machine learning based approaches have also been used  
73 to cluster drugs or diseases and predicting new drug activity and usage.<sup>33-37</sup> Methods for  
74 finding novel uses of drugs based on analysis of biomedical literature,<sup>38,39</sup> electronic health  
75 records,<sup>37,40</sup> and biological networks<sup>41,42</sup> have also been reported.

## 76 **Drug similarity**

77 Implementations of drug discovery and drug repurposing sometimes rely on the principle of  
78 similar molecules having similar properties.<sup>43,44</sup> In drug design, repurposing, or screening,  
79 similar compounds are generally assumed to have similar molecular targets. In structure-  
80 based drug discovery, if two potential molecular targets are identified as similar, then a  
81 compound that modulates one target is inferred to modulate the other. In ligand-based  
82 methods, similar compounds are inferred to analogously modulate the behavior of the same  
83 target(s). In our computational shotgun drug repurposing experiments, we extend the sim-  
84 ilarity property principle to examining interactions on a proteomic scale. Compounds with  
85 similar proteomic interaction signatures are hypothesized to be effective for the same indi-  
86 cation(s).

## 87 **Shotgun drug repurposing with CANDO**

88 The goal of the Computational Analysis of Novel Drug Opportunities (CANDO) platform  
89 for shotgun drug discovery and repurposing is to screen every human use compound/drug  
90 against every indication/disease.<sup>45-48</sup> The tenets of CANDO include docking with dynamics,  
91 multitargeting, and shotgun repurposing, which have been developed over the last decade

92 and a half.<sup>49-51</sup> The first version of CANDO (v1) applied a bioinformatic docking protocol  
93 on large libraries of compound and protein structures. The multitargeting nature of drugs<sup>52</sup>  
94 is captured by inferring their similarity on a proteomic scale after calculating interactions  
95 between all compounds and all proteins in the corresponding libraries.<sup>8,45,46</sup> This is key, as in-  
96 dications can be multifactorial in nature, involving disparate or intertwined pathways.<sup>53? -56</sup>  
97 Similar compounds, as determined by the root mean square deviation (RMSD) of their pro-  
98 teomic interaction signatures, are hypothesized to behave similarly, i.e., compounds which  
99 are ranked highly (most similar compound-proteome interaction signatures) to a drug with  
100 an approved indication are hypothesized to be repurposable drugs/compounds for that indi-  
101 cation. Benchmarking is accomplished by examining the ranks of other approved drugs for  
102 the same indication.<sup>45,46</sup>

103 There exist other approaches to determine compound similarity without the need for  
104 docking calculations. Different representations of molecules capture different chemical, phys-  
105 ical, or functional aspects of a compound. Two or three dimensional molecular fingerprints  
106 are used in the field of cheminformatics to describe compounds.<sup>57</sup> In these models, the phys-  
107 ical arrangement of atoms in a compound is captured as a binary vector where each entry of  
108 a vector indicates the presence or absence of a specific molecular feature.<sup>44</sup> A distance (sim-  
109 ilarity) metric between these vectors can be measured, using metrics such as the Tanimoto  
110 coefficient, a widely used metric in medicinal chemistry and ligand-based virtual screen-  
111 ing.<sup>44,58-60</sup> This is analogous to the structure-based methods used to construct interaction  
112 signatures in v1 and the RMSD measure used to calculate similarity.

113 In this study, we extend CANDO to include ligand-based drug repurposing by creating  
114 new pipelines based on identifying compound similarity based on their molecular finger-  
115 prints, as well as data fusion pipelines that combine the protein-centric and protein-agnostic  
116 approaches. The new ligand-based pipelines in CANDO are based on molecular fingerprint  
117 similarity calculations using the Research Development Kit (RDKit),<sup>61</sup> and are not meant  
118 as an exhaustive exploration of all possible CANDO pipelines that can be built using all the

119 fingerprint descriptions available from RDKit. Instead, we constructed pipelines using well  
120 studied molecular fingerprints<sup>62</sup> to evaluate feasibility and compare and contrast benchmark-  
121 ing performance. Using the standard CANDO benchmarking procedure (see “Methods”),  
122 several of the pipelines described here yielded better performance than those previously  
123 obtained using v1 by itself.

124       Combination of other pipelines using data fusion as well as a decision tree approach be-  
125 tween v1 and the best performing ligand-based approach (“ECFP4”) yielded better bench-  
126 marking performance than using either pipeline by itself, allowing for increased accuracy  
127 while retaining the mechanistic and precision medicine opportunities afforded by the protein-  
128 centric approach of v1. Higher benchmarking accuracies are indicative of higher drug repur-  
129 posing potential, increased confidence in our predictions, a decreased number of compounds  
130 which must be tested in wet lab experiments and clinical trials to obtain true hits, and thus  
131 less time and cost required to find a new use for an old drug.

## 132 **Methods**

133 Figure 1 illustrates the different pipelines evaluated in this study, which are described in  
134 detail below.

### 135 **The CANDO platform and the version 1 (v1) pipeline**

136 A detailed description of the CANDO platform, including the v1 pipeline used for assigning  
137 drugs to indications, as well as its benchmarking performance, is available elsewhere.<sup>45–47,63</sup>

138 Briefly, in v1 we predicted interactions between 46784 protein structures and 3733 small  
139 molecules that mapped to 2030 indications. We obtained the molecular structures of the  
140 3733 small molecules in our putative drug library from the Food and Drug Administra-  
141 tion (FDA), NCATS Chemical Genomics Center, and PubChem.<sup>64</sup> Solved x-ray diffraction  
142 structures of proteins were obtained from the Protein Data Bank<sup>65</sup> and modeled protein

143 structures were generated using I-TASSER.<sup>19</sup> Approved drug-indication associations were  
144 obtained from the Comparative Toxicogenomics Database (CTD)<sup>66</sup> and mapped to the  
145 CANDO drug library, resulting in 2030 indications with at least one approved/associated  
146 compound. Protein-compound interaction scores were calculated using a bio- and chem-  
147 informatic docking protocol consisting of ligand binding site identification for all proteins  
148 in our structure library, followed by similarity measurement between known ligands in the  
149 identified binding sites and all 3733 compounds in our putative drug library.<sup>46</sup> A compound  
150 is characterized as an “interaction signature” of length 46784, where each entry is an inter-  
151 action score between 0 - 2, indicating the strength of a predicted protein interaction (zero  
152 signifying no interaction). Each compound is then compared to every other compound by  
153 calculating the root mean square deviation (RMSD) between the corresponding interaction  
154 signatures, generating a compound-compound (or drug-compound) similarity matrix. Each  
155 compound is ranked relative to every other compound in order of increasing similarity and  
156 benchmarking performed.

## 157 **Ligand-based pipelines**

158 The CANDO platform for shotgun drug repurposing is not dependent on any particular  
159 method for determining compound similarity, such as the protein-centric one used in v1.  
160 Here, we consider the utility of ligand-based pipelines by constructing two dimensional  
161 molecular fingerprints of the 3733 compounds in the CANDO putative drug library using the  
162 open-source cheminformatics software RDKit Python API<sup>30</sup> and performing an all-against-  
163 all comparison using the Tanimoto coefficient. Once the features of a molecule have been  
164 quantized into a vector, the Tanimoto coefficient is a score of how many bits two vectors have  
165 in common divided by the number of bits by which they differ, i.e.,  $|A \cap B|/|A \cup B|$ , where  
166 A and B represent compounds in binary vector form, and  $|A|$  is the length of the vector.

167 For efficiency and accuracy, we described our putative drug library using well studied  
168 2D molecular fingerprints.<sup>44</sup> Specifically, we used Morgan fingerprints,<sup>67</sup> otherwise known

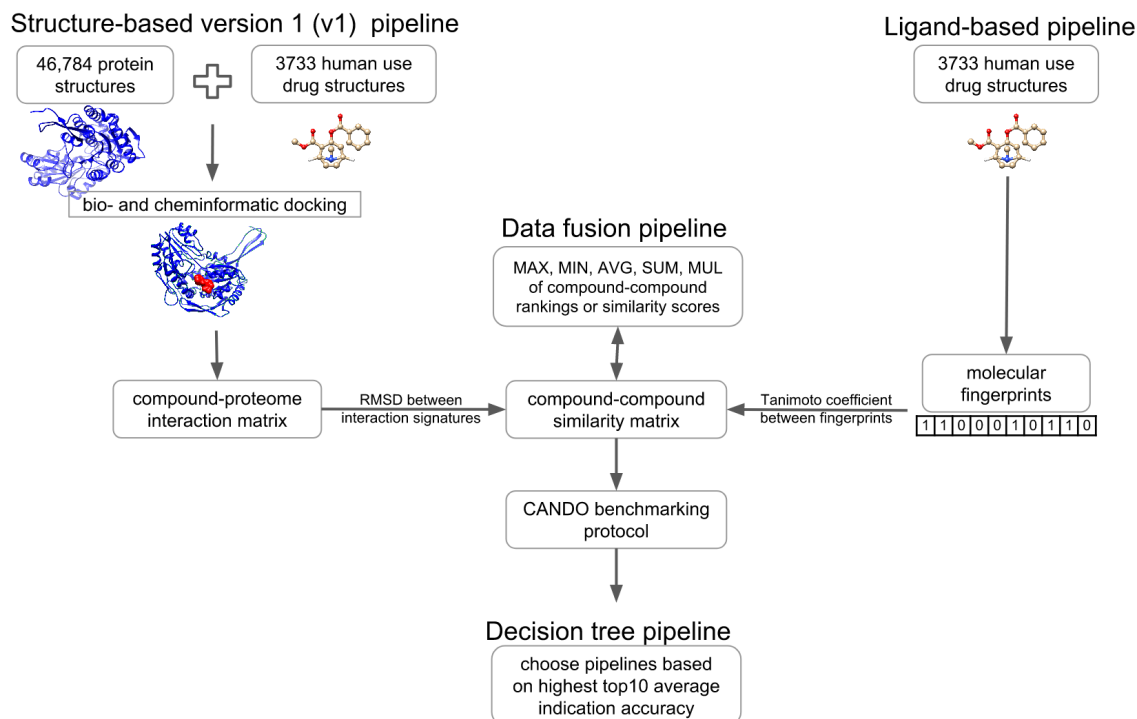


Figure 1: **Flow diagram of the CANDO platform pipelines used for shotgun drug repurposing.** The v1 structure-based pipeline is the original protein-centric approach based on a bioinformatic docking protocol used to construct compound-proteome interaction signatures. The ligand-based pipelines are based on molecular fingerprint representations of compounds. The data fusion pipelines consist of a combination these two types of pipelines after calculating compound-compound similarity, and the decision tree pipeline is devised based on the performance of individual structure- and ligand-based pipelines (see Methods). All pipelines, except the decision tree pipeline, generate a compound-compound similarity matrix that is sorted and ranked. These rankings are used to generate putative repurposable drug candidates and evaluate benchmarking performance. The figure illustrates the utility of implementing, as well as comparing and contrasting, multiple (types of) pipelines in the CANDO platform for shotgun drug repurposing.

169 as Extended Connectivity Fingerprints (ECFP, a circular fingerprint), one Functional Class  
170 Fingerprint (FCFP, a functional class fingerprint<sup>68</sup>), and fingerprints from RDKit (RDKit, a  
171 linear fingerprint). Circular fingerprints are bit vector representations of compounds encod-  
172 ing the presence of molecular substructures constructed outward from all starting positions  
173 (all atoms) in a radial fashion; functional class fingerprints are binary vectors which encode  
174 the presence of predefined “functional” features of a compound; and linear fingerprints en-  
175 code the presence of molecular substructures built in a linear fashion from all possible starting



176 points (all atoms).<sup>62</sup>

177 All fingerprints are additionally described by the length of the molecular substructure  
178 (“radius” or “diameter” depending on the type and implementation) captured. For in-  
179 stance, ECFP4 is a fingerprint created using ECFP with diameter four. Specific ligand-  
180 based pipelines in CANDO are identified according to the molecular fingerprint used, i.e.,  
181 “ECFP4” refers to the CANDO pipeline where compounds are represented using the ECFP4  
182 molecular fingerprint.

183 Hert et al. found the optimal results for quantifying relationships between drug classes  
184 was achieved using ECFP4 fingerprints with similarities calculated using the Tanimoto coeffi-  
185 cient.<sup>59</sup> We extended this to ligand-based drug repurposing using vectors of 2048 bits instead  
186 of the 1024 used in.<sup>59</sup> We calculated the Tanimoto coefficient between the fingerprints of all  
187 possible pairs of the 3733 compounds in our library, and used this to populate a compound-  
188 compound similarity matrix, just as we did with the v1 pipeline, allowing us to sort and  
189 rank all compounds relative to each other. Fingerprints could not be created for twelve of  
190 the 3733 compounds in our putative drug library, which were generally large compounds  
191 with metal chelation or long polymers. We then evaluated benchmarking performance of the  
192 ligand-based pipelines as described further below.

### 193 **Data fusion pipelines**

194 We combined rankings from the v1 pipeline with the new molecular fingerprint rankings using  
195 one of the following criteria: lower of two rankings (MIN), higher of two rankings (MAX),  
196 sum of two rankings (SUM), average of two rankings (AVG). This is known as “rank-based  
197 data fusion”.<sup>69</sup> We also combined the compound-compound similarity scores from v1 and  
198 the ligand-based pipelines using the multiplication of raw similarity scores (MUL), a type of  
199 “kernel-based data fusion”.<sup>69</sup> After multiplying the similarity scores from two pipelines, the  
200 compounds are sorted and ranked based on the newly calculated scores. As in v1 and the  
201 ligand-based pipelines, the compound-compound rankings from these data fusion pipelines

202 is then subjected to benchmarking.

### 203 **Decision tree pipeline**

204 A goal of CANDO is to make predictions of which compounds are likely to be efficacious  
205 against any particular indication. A second is to use analytics to identify causal relationships  
206 that predict indication etiology. From the benchmarking, we can determine *a priori* the  
207 pipeline that has the best performance for a particular indication, which are then used to  
208 generate putative drug candidates for that indication. We constructed a new meta pipeline  
209 that makes a decision as to optimal performance on a per indication basis. We made this  
210 decision using the top10 average indication accuracy metric (described below), from two  
211 choices, v1 and the best performing ligand-based pipeline, namely ECFP4 (see Results). We  
212 used this to create a merged set of data which was then benchmarked. For example, the  
213 v1 pipeline yields a top10 average indication accuracy of 25% for type 2 diabetes, whereas  
214 ECFP4 yields a top10 accuracy of 35%. In the combined decision tree pipeline, we choose  
215 to use ECFP4 for the prediction of repurposing candidates for type 2 diabetes, and for the  
216 calculation of all benchmarking performance metrics at all cutoffs. We extended this method  
217 of choosing the pipeline (between v1 and ECFP4) with higher top10 average indication  
218 accuracy to all indications. This aligns with the logic that a clinician or researcher using  
219 CANDO can choose the pipeline with the highest accuracy for a particular indication, which  
220 is reflected in the benchmarking performance of this combined pipeline.

### 221 **Benchmarking pipelines in the CANDO platform**

222 Three measures are used to perform the leave-one-out benchmarking of the CANDO platform  
223 pipelines: average indication accuracy, pairwise accuracy, and coverage. Average indication  
224 accuracy (%) evaluates the likelihood of capturing at least one drug mapped to the same  
225 indication within a particular cutoff from the list of compounds ranked in order of similarity,  
226 which is averaged over the 1439 indications with at least two approved drugs and expressed

227 as a percent. Mathematically, this is expressed as  $c/d \times 100$ , where  $c$  is the number of times  
228 at least one other drug approved for the same indication was captured within a cutoff and  $d$   
229 is the total number of drugs approved for that indication. The top10, top25, top1% (top37),  
230 top50, and top100 cutoffs are used, signifying the top ranking 10-100 similar compounds.  
231 In other words, the indication accuracy represents the recovery rate of known drugs for  
232 a particular indication, which is then averaged across all 1439 indications with at least  
233 two approved drugs. Pairwise accuracy (%) is the weighted average of the per indication  
234 accuracies based on the number of compounds approved for a given indication. Coverage is  
235 the number of indications with non-zero accuracy expressed as a percent.

## 236 **Controls**

237 The performance of a given pipeline is evaluated relative to a random control, which is the  
238 result that we would expect by chance. The original random control data for v1 was generated  
239 by repeated creation of random compound-proteome interaction matrices by sampling from  
240 the distribution of values present in the v1 matrix. The benchmarking performance for  
241 these random control matrices was calculated as described above and in.<sup>46,63</sup> However, the  
242 new ligand centric pipeline is protein agnostic, and the data fusion ones consist of protein  
243 agnostic components. Therefore, we constructed a compound-compound matrix of uniformly  
244 random similarity scores to use as controls in this study, i.e., the similarity between any two  
245 compounds was assigned a random value between 0 and 1. We sorted and ranked every  
246 compound relative to every other compound using this this random compound-compound  
247 similarity matrix, and evaluated benchmarking performance as described above.

## 248 Results

### 249 Benchmarking performance of the different pipelines

250 The new pipelines (Figure 1) generally outperform v1 for all three metrics used to evalu-  
251 ate benchmarking performance: average indication accuracy, pairwise accuracy, and coverage  
252 (Figure 2). The MUL:v1,ECFP4 data fusion pipeline, created by multiplying the compound-  
253 compound similarity scores (RMSD of interaction signatures) from v1 with the Tanimoto  
254 coefficient measured between the compounds described using the ECFP4 molecular finger-  
255 print, yields the overall best performance relative to v1 and the ones based on fingerprint  
256 comparisons. Specifically, we obtained the highest top10, top25, and top50 average indi-  
257 cation accuracies of 17.3%, 23.8%, and 29.6% using this data fusion pipeline. The highest  
258 top1% (or top37) and top100 average indication accuracies of 26.8% and 36.7% were ob-  
259 tained using the pipeline based on the ECFP4 molecular fingerprints. Most of the molecular  
260 fingerprint pipelines outperform the original v1 pipeline with the exception of ECFP0, a  
261 fingerprint based on simple atom count quantization (Figure 2).

262 The decision tree meta pipeline, built by combining other pipelines based on the cor-  
263 responding top10 average indication accuracies, yields accuracies of 19.0%, 25.7%, 28.3%,  
264 31.4%, and 39.1% at the five cutoffs used. In contrast, the best performing control generated  
265 from uniformly random compound-compound similarity data obtains average indication ac-  
266 curacies of 2.2% at the top10 cutoff, the most stringent one used to benchmark the CANDO  
267 platform (Figure 2).

268 In terms of pairwise accuracy (%), which is the weighted average of the per indication  
269 accuracies based on the number of compounds approved for a given indication (see Methods),  
270 ECFP4 outperforms all other pipelines, including the decision tree, with accuracies of 28.5%,  
271 38.9%, 43.8%, 47.9%, and 58.8% at the five cutoffs.

272 The coverage metric evaluates the fraction (or percentage) of the 1439 indications with  
273 two approved drugs for which there is at least one instance of a successful recapture or

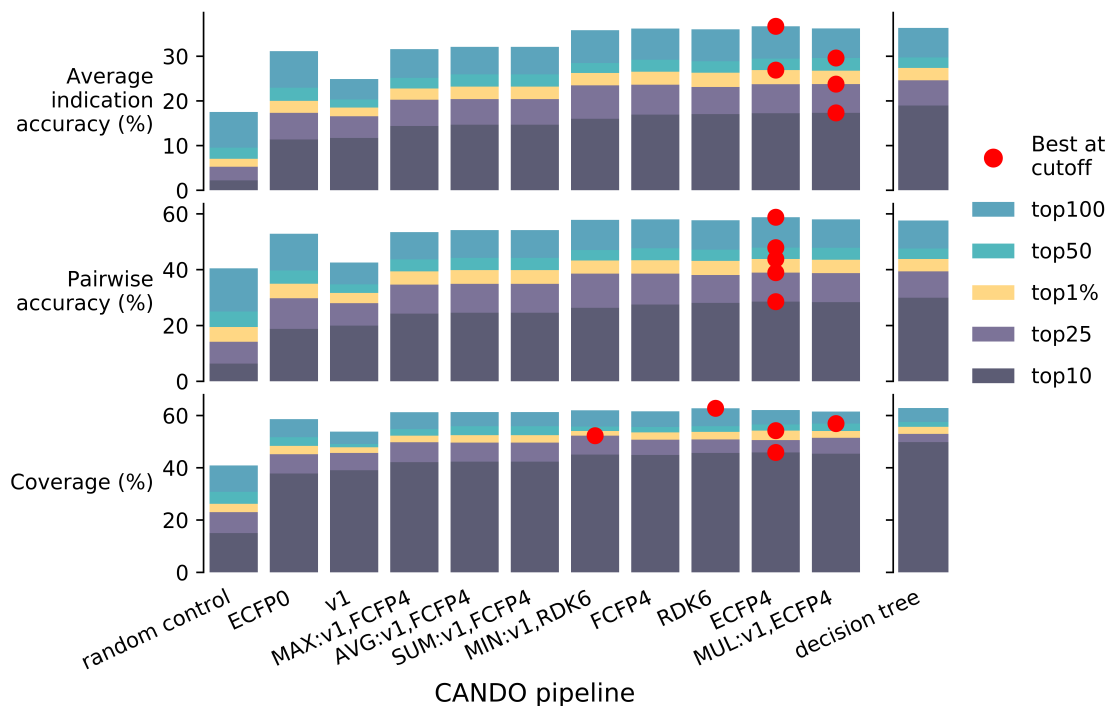


Figure 2: **Benchmarking performance of different CANDO platform pipelines.** The average indication accuracy (top), pairwise accuracy (middle), and coverage (bottom) for each pipeline are shown at different cutoffs. The value for the top10 cutoff is denoted by dark purple, top25 by light purple, top1% (or top37) by yellow, top50 by green, and top100 by light blue. The individual pipeline with the best performance at each each cutoff is denoted by a red dot. The meta decision tree pipeline was built combining two pipelines, v1 and ECFP4, using the top10 average indication accuracy and so has the highest top10 accuracy and coverage, but is excluded by the “Best at cutoff” marker. The pipelines in all plots are sorted according to increasing top10 average indication accuracy, the most stringent criteria used in our benchmarking. The MUL:v1,ECFP4 pipeline yields the overall best performance relative to the other individual structure- and ligand-based pipelines. The pipeline based on the ECFP4 molecular fingerprint produces the highest top1% and top100 average indication accuracies (top). When assessing pairwise accuracy (middle), ECFP4 is the best performing individual pipeline. The coverage (bottom) plot is a percentage of the 1439 indications for which a pipeline produces a non-zero indication accuracy. The data fusion pipelines of MUL:v1,ECFP4 and MIN:v1,RDK6 have the highest coverage at the top50 and top25 cutoffs, the ECFP4 at the top10 and top50 cutoffs, and RDK6 at the top100 cutoff. Overall, the pipelines using molecular fingerprints have promise and potential for shotgun drug repurposing by themselves, but the data fusion and decision tree pipelines that combine structure-based and ligand-based approaches achieve the best performance while retaining the benefits of both types of approaches.

274 recovery of the known drug within a particular cutoff. The ECFP4 pipeline has the highest  
 275 top10 and top1% coverage of 45.9% and 54.2%, the MIN:v1,RDK6 yields the highest top25

276 coverage of 52.3%, the MUL:v1,ECFP4 has the highest coverage at the top50 cutoff of 56.9%,  
277 and RDK6 the highest at the top100 cutoff of 62.8%. In contrast, the decision tree pipeline,  
278 built in part to increase coverage, has a top10 coverage of 49.8%. This means that for almost  
279 half of all the 1439 indications, we capture a drug associated with that indication within the  
280 top10 cutoff (Figure 2).

## 281 **Distribution of indication accuracies between the two types of pipelines**

282 To compare and contrast the behavior of the structure-based and ligand-based pipelines,  
283 we calculated histograms of the average indication accuracies and counts of the highest per  
284 indication accuracies at each cutoff for two pipelines (v1 and ECFP4), excluding indications  
285 for which a 0% average indication accuracy is obtained. Figure 3 shows that the ECFP4  
286 pipeline has more indications with higher accuracies than v1 (the yellow histogram is shifted  
287 to the right of the purple histogram). The Kolmogorov–Smirnov statistical test p-values  
288 shown in the corresponding left hand side graph of Figure 3 indicate that the distributions  
289 of the v1 and ECFP4 accuracies are drawn from different samples in a statistically significant  
290 manner. The Venn diagrams of the 1439 indications in CANDO with more than one approved  
291 drug shows that v1 obtains a higher top10 accuracy for 150 indications, while ECFP4 obtains  
292 a higher top10 accuracy for 445, and 122 indications have the same non-zero top10 accuracy  
293 for both pipelines. As the cutoff increases, more indications have higher accuracies using  
294 the ECFP4 pipeline relative to v1, while the number of indications with the same accuracy  
295 increases relatively. The orthogonality in the histograms and Venn diagrams indicate that  
296 both types of pipelines appear necessary for maximum coverage and accuracy across all the  
297 indications. Figure 3 also suggests that additional pipelines and/or improvement in existing  
298 pipelines is necessary to recover drugs for  $\approx 500$  indications that are not covered by either  
299 pipeline at the highest cutoff.

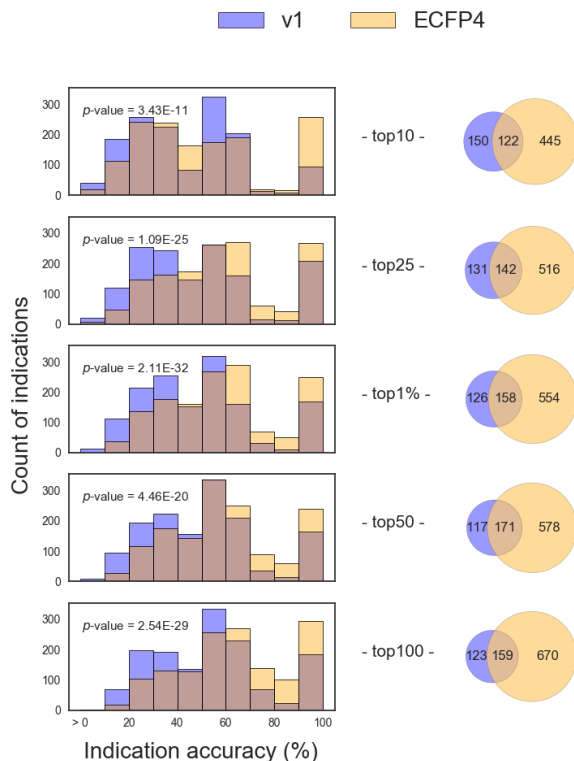


Figure 3: **Comparison and overlap of indication accuracy distributions for two CANDO platform pipelines at different cutoffs.** The left hand side shows the histograms of the counts of indications with a particular average indication accuracy (or accuracy distributions) for two pipelines, v1 (purple) and ECFP4 (yellow). Indications where both pipelines perform equally well are indicated by brown. For example, at the top10 cutoff, there are approximately 200 indications which achieve an average accuracy between 10 and 20% using the v1 pipeline but just over 100 using ECFP4. At all cutoffs, a greater number of indications with higher accuracies is observed for the ECFP4 pipeline (increase in yellow along the horizontal axis). The  $p$ -value, derived from the Kolmogorov-Smirnov test statistic applied to the two distributions at each cutoff, indicates that they are significantly different. On the right hand side of the figure are Venn diagrams of the set of indications with higher accuracies at each cutoff (excluding indications with 0% accuracy). For example, at the top10 cutoff, there are 150 indications for which the v1 pipeline yields higher average indication accuracies, 445 for which the ECFP4 pipeline is higher, and 122 with the same performance. The ECFP4 pipeline performs better than v1 for more indications at all cutoffs, but both pipelines appear to be necessary to achieve the best performance across all indications for shotgun drug repurposing.

### 300 Putative drug candidate generation and validation

301 The top ranking putative drug candidates generated by the v1 pipeline for eight indications,  
 302 tuberculosis, malaria, hepatitis B, hepatitis C, systemic lupus erythematosus, type 2 diabetes

303 mellitus, and Alzheimer’s disease, are available from Figure 3 and Supplementary Material  
304 of a previous publication.<sup>45</sup> The top candidates were chosen based on a concurrence score  
305 which is “the number of occurrences of particular compounds in each set of top 25 predictions  
306 generated for all of the drugs approved for a particular indication”.<sup>45</sup> Using this concurrence  
307 score measure, we generated the top candidate drugs to treat the same indications with  
308 the ECFP4 molecular fingerprint and the MUL:v1,ECFP4 data fusion pipelines. We then  
309 searched the biomedical literature using PubMed and Google Scholar for published studies  
310 corroborating these top candidates.

311 Both of the new pipelines predict colistin (polymyxin E) as a treatment for tuberculosis,  
312 which has been studied as a potentiator of anti-tuberculosis drugs.<sup>70</sup> Minocycline was a top  
313 result from both pipelines for malaria, which has been shown to protect against certain types  
314 and complications.<sup>71</sup> However, the CDC recommends using doxycycline and not minocycline  
315 as malaria prophylaxis.<sup>72</sup> Additionally, for malaria, both new pipelines list tigecycline among  
316 the top ranked candidates, which has shown antimalarial activity in preclinical studies.<sup>73,74</sup>

317 All three pipelines recommend known antivirals for hepatitis B. For hepatitis C, all  
318 three pipelines list didanosine in the top ranked candidates. Unfortunately, concurrent use  
319 of didanosine and traditional hepatitis treatments may induce dangerous consequences for  
320 the patient,<sup>75</sup> illustrating the need for careful expert curation of top candidates generated  
321 by the CANDO platform. For Alzheimer’s disease, one of the highest scoring compounds  
322 from the MUL:v1,ECFP4 pipeline was dextromethorphan. In 2015, a study was published  
323 showing dextromethorphan hydrobromide–quinidine sulfate was well tolerated in patients  
324 with Alzheimer’s disease and had clinically relevant efficacy in treating patients, as mea-  
325 sured via agitation.<sup>76</sup> These examples indicate new putative drug candidate generation by  
326 the CANDO platform with these integrated pipelines is likely to work as well, if not bet-  
327 ter, relative to the prospective validation studies previously done using v1 or its compo-  
328 nents.<sup>8,50,77–80</sup> The full list of drug candidates for the above indications based on the concur-  
329 rence score using the newer pipelines are given in the Supporting Information and available



330 at [http://protinfo.org/cando/results/fingerprinting\\_cando](http://protinfo.org/cando/results/fingerprinting_cando). Putative drug candi-  
331 date predictions for all 2030 indications in the platform using the v1 pipeline are available  
332 at <http://protinfo.org/cando/data/raw/matrix/>.

## 333 Discussion

### 334 Interpretation of results

335 Higher benchmarking accuracies are expected to result in better drug repurposing predic-  
336 tions. The top ranked similar compounds to the known drugs for a particular indication  
337 using the pipeline with the best benchmarking performance is expected to produce hits and  
338 leads with the highest likelihood of success when validated in downstream preclinical and  
339 clinical studies. The decreased need to test a large number of compounds with the new  
340 pipelines, along with greater confidence in the computational models of drug-indication as-  
341 sociations, realizes the goal of drug repurposing: making drug discovery more efficient by  
342 reducing the labor, time, and risk in finding new uses for existing therapeutics.

343 Using the new pipelines based on molecular fingerprinting and data fusion with v1 (Fig-  
344 ure 1), we obtain better benchmarking performance than using v1 by itself (Figure 2). Our  
345 cutoffs for calculating performance metrics are chosen based on collaborations with wet lab  
346 experimentalists willing to test the top candidates generated by our CANDO platform for  
347 particular indications. In practice, when working with preclinical and clinical collaborators,  
348 we currently employ the decision tree approach of selecting the pipeline with the highest  
349 accuracy for a specific indication and the desired cutoff. For example, if a collaborator is ca-  
350 pable of validating ten candidates for Precursor B-Cell Lymphoblastic Leukemia-Lymphoma  
351 (MeSH identifier D015452), which is one of the 150 where the benchmarking performance  
352 is better using the v1 pipeline relative to ECFP4, then we would use the former pipeline to  
353 generate the top ten putative drug candidates for this indication.

354 The new integrated pipelines also yield a higher number of indications covered relative to

355 v1, i.e., more indications with a non-zero accuracy, demonstrating their generalized utility  
356 for shotgun drug repurposing. Indication-specific validation studies may rely on the pipeline  
357 with highest accuracy for that indication, but CANDO platform development in shotgun drug  
358 repurposing requires that the coverage also increase in addition to the average indication and  
359 pairwise accuracy. The best performing random control achieves a top10 average indication  
360 accuracy of 2.2%, and the random control based on random sampling from the distribution  
361 the v1 compound-protein interaction matrix values yielded a top10 accuracy of 0.2%.<sup>45,46</sup>  
362 These random control accuracies are at least an order of magnitude lower than the accuracies  
363 obtained using the newer pipelines, and align with expected hit rates in high throughput  
364 screening.<sup>81</sup> All pipelines yield better performance when compared to the random control  
365 (Figure 2), and the differences between the performances of the different pipelines and that  
366 of the control signify the value added by our chosen approaches. The orthogonality in the  
367 histograms and Venn diagrams of Figure 3 indicate that both types of pipelines appear  
368 necessary for maximum coverage and accuracy across all the indications.

### 369 **Limitations and future work**

370 We have added new pipelines based on ligand-based fingerprint comparisons to the CANDO  
371 platform (Figure 1) that increase benchmarking performance relative to the original v1  
372 protein-centric pipeline (Figure 2). We are further enhancing CANDO by improving the per-  
373 formance of existing pipelines via parameter optimization,<sup>82</sup> exploration of different docking  
374 approaches to generate the compound-proteome interaction signatures,<sup>83</sup> adding new orthog-  
375 onal pipelines based on compound-pathway signatures,<sup>63</sup> implementing more sophisticated  
376 data fusion and machine learning approaches, and by continued dissection of the features  
377 responsible for pipeline performance and behavior.<sup>46,47,63</sup>

378 Notwithstanding the relative benchmarking performance of the existing CANDO plat-  
379 form pipelines, the structure-based virtual screening or protein docking pipelines are not  
380 without their merits. The protein-centric approach enables mechanistic understanding of

381 drug action by modeling compound-protein interactions at the atomic level. Additionally,  
382 the protein-centric approach readily lends itself to problems in precision medicine/drug re-  
383 purposing: Incorporating genetic changes, and modeling amino acid mutations due to non-  
384 synonymous nucleotide polymorphisms in protein structures, will result in altered compound-  
385 protein interaction scores, allowing us to tailor drug repurposing candidates to an individual  
386 genome/proteome. The protein-centric approach facilitates consideration of polypharmacy,  
387 where the cumulative effects of multiple drugs on protein targets can be evaluated by the  
388 analysis and integration of the corresponding drug-proteome interaction signatures, which  
389 can then be used to generate putative drug cocktails and combination therapy candidates.  
390 The protein-centric pipeline may also be used to generate putative drug candidates for indi-  
391 cations without any approved drugs, but where the target protein or proteome is known.<sup>8</sup>

392 We are continuing to enhance the virtual screening pipelines to model reality more ac-  
393 curately, with the goal of increasing compound-proteome signature comparison accuracy.  
394 For instance, we are exploring the use different molecular docking programs, such as CAN-  
395 DOCK<sup>84,85</sup> and AutoDock Vina,<sup>86</sup> to populate the compound-proteome interaction signa-  
396 tures. An updated version of the v1 pipeline, v1.5, with parameters optimized for scoring  
397 compound-proteome interactions, yields benchmarking performance that is 10% higher rela-  
398 tively at the top10 cutoff (12.8% for v1.5 versus 11.7% for v1).<sup>82</sup> By combining the improved  
399 protein centric and protein agnostic pipelines using data fusion, we obtain the best perfor-  
400 mance and retain the benefits of both types of approaches, while minimizing the weaknesses  
401 of any single approach.

402 The higher benchmarking performance obtained by the ligand-based pipelines may in  
403 part be due to the nature of drug discovery and development, which is biased in favor  
404 of already effective compounds in an effort to break into a new market or retain market  
405 dominance by generating new intellectual property. New drugs are often derivatives of  
406 existing ones with small changes.<sup>87,88</sup> Repurposing based on molecular fingerprint similarity  
407 will be highly enriched for these “me too” compounds,<sup>88</sup> given that the approach to shotgun

408 drug repurposing in the CANDO platform is currently based on detecting drug-compound  
409 similarities.

410 Our benchmarking performance metrics are biased toward reporting particular pipelines  
411 as better when they capture what is already known/approved, and not novel repurposing  
412 candidates which will work to treat or cure an indication in reality. Barring large scale  
413 preclinical validation of putative drug candidates, it remains a reproducible and a meaningful  
414 measure in our studies.<sup>45–47</sup>

415 Our goal in this study was to assess the value of adding fingerprinting and data fusion  
416 pipelines to the existing protein-centric pipelines in the CANDO platform, and not an ex-  
417 haustive enumeration, comparison, and fusion of ligand- and structure-based approaches for  
418 identifying drug associations.<sup>89</sup> More sophisticated fingerprint representations encode the  
419 structures of compounds differently and capture unique features particularly of relevance  
420 to drug discovery and repurposing. Future work will extend our analyses to include ad-  
421 ditional fingerprints that can be created using RDKit, including the Long Extended and  
422 Feature Connectivity Fingerprints (LECFP and LFCFP, respectively). Longer fingerprints  
423 have been shown to better describe a compound with less redundancy, leading to increased  
424 accuracy in virtual screening.<sup>90</sup>

425 Features and categories of indications, proteins, and compounds all influence the drug  
426 repurposing accuracy of CANDO. We are continuing to undertake thorough experiments  
427 exploring the roles of particular features responsible for benchmarking performance.<sup>46,47,63</sup>  
428 Incorporating machine learning to understand how compound-proteome interaction signa-  
429 tures influence performance will help us find the most parsimonious molecular descriptors  
430 for compounds. Drugs may have targets beyond proteins, including DNA and RNA.<sup>91,92</sup>  
431 To better model how a compound interacts with all potential targets, we are integrating  
432 compound-nucleic acid interaction modeling into CANDO. Finally, we are working with col-  
433 laborators to validate the predictions from the various pipelines in preclinical and clinical  
434 studies, which represents the ultimate test of the CANDO platform.

## 435 **Conclusions**

436 CANDO is a computational platform for shotgun drug discovery and repurposing. We imple-  
437 mented new ligand-based and data fusion pipelines in the CANDO platform, and obtained  
438 substantial improvement in benchmarking performance using a combination of protein-  
439 centric and protein-agnostic methods. These improved results indicate greater confidence  
440 in drug repurposing predictions made by us using CANDO and demonstrate the value of  
441 considering different, orthogonal, types of approaches for calculating compound-compound  
442 similarities. Our integrated approach moves us closer to developing an accurate, robust,  
443 and reliable computational drug repurposing platform, and using it to understand how small  
444 molecules interact with each other and with larger macromolecules in their corresponding  
445 environments.

## 446 **Acknowledgement**

447 This work was supported in part by a National Institute of Health Director's Pioneer Award  
448 (DP1OD006779), a National Institute of Health Clinical and Translational Sciences Award  
449 (UL1TR001412), and startup funds from the Department of Biomedical Informatics at the  
450 University at Buffalo.

451 The authors thank Dr. Zackary Falls, William Mangione, Matt Hudson, and Dr. Manoj  
452 Mammen for their contributions to this project, including software development, and manuscript  
453 reading.

## 454 **Supporting Information Available**

455 All Supporting Information about this project can be found at [http://protinfo.org/  
456 cando/results/fingerprinting\\_cando](http://protinfo.org/cando/results/fingerprinting_cando).

## 457 References

- 458 (1) Prasad, V.; Mailankody, S. Research and development spending to bring a single cancer  
459 drug to market and revenues after approval. *JAMA internal medicine* **2017**, *177*, 1569–  
460 1575.
- 461 (2) Ashburn, T. T.; Thor, K. B. Drug repositioning: identifying and developing new uses  
462 for existing drugs. *Nature reviews Drug discovery* **2004**, *3*, 673.
- 463 (3) Langedijk, J.; Mantel-Teeuwisse, A. K.; Slijkerman, D. S.; Schutjens, M.-H. D. Drug  
464 repositioning and repurposing: terminology and definitions in literature. *Drug discovery*  
465 *today* **2015**, *20*, 1027–1034.
- 466 (4) Palumbo, A.; Facon, T.; Sonneveld, P.; Blade, J.; Offidani, M.; Gay, F.; Moreau, P.;  
467 Waage, A.; Spencer, A. et al. Thalidomide for treatment of multiple myeloma: 10 years  
468 later. *Blood* **2008**, *111*, 3968–3977.
- 469 (5) Sardana, D.; Zhu, C.; Zhang, M.; Gudivada, R. C.; Yang, L.; Jegga, A. G. Drug  
470 repositioning for orphan diseases. *Briefings in bioinformatics* **2011**, *12*, 346–356.
- 471 (6) Li, J. J.; Johnson, D. S. *Modern drug synthesis*; John Wiley & Sons, 2013.
- 472 (7) Kouznetsova, J.; Sun, W.; Martínez-Romero, C.; Tawa, G.; Shinn, P.; Chen, C. Z.;  
473 Schimmer, A.; Sanderson, P.; McKew, J. C. et al. Identification of 53 compounds  
474 that block Ebola virus-like particle entry via a repurposing screen of approved drugs.  
475 *Emerging microbes & infections* **2014**, *3*, e84.
- 476 (8) Chopra, G.; Kaushik, S.; Elkin, P. L.; Samudrala, R. Combating ebola with repurposed  
477 therapeutics using the CANDOR platform. *Molecules* **2016**, *21*, 1537.
- 478 (9) Schuler, J.; Hudson, M. L.; Schwartz, D.; Samudrala, R. A Systematic Review of Com-  
479 putational Drug Discovery, Development, and Repurposing for Ebola Virus Disease  
480 Treatment. *Molecules* **2017**, *22*, 1777.

- 481 (10) Bertolini, F.; Sukhatme, V. P.; Bouche, G. Drug repurposing in oncology—patient and  
482 health systems opportunities. *Nature Reviews Clinical Oncology* **2015**, *12*, 732.
- 483 (11) Corbett, A.; Pickett, J.; Burns, A.; Corcoran, J.; Dunnett, S. B.; Edison, P.; Ha-  
484 gan, J. J.; Holmes, C.; Jones, E. et al. Drug repositioning for Alzheimer’s disease.  
485 *Nature Reviews Drug Discovery* **2012**, *11*, 833.
- 486 (12) Zheng, W.; Thorne, N.; McKew, J. C. Phenotypic screens as a renewed approach for  
487 drug discovery. *Drug discovery today* **2013**, *18*, 1067–1073.
- 488 (13) Xu, M.; Lee, E. M.; Wen, Z.; Cheng, Y.; Huang, W.-K.; Qian, X.; Julia, T.;  
489 Kouznetsova, J.; Ogden, S. C. et al. Identification of small-molecule inhibitors of Zika  
490 virus infection and induced neural cell death via a drug repurposing screen. *Nature*  
491 *medicine* **2016**, *22*, 1101.
- 492 (14) Aparoy, P.; Kumar Reddy, K.; Reddanna, P. Structure and ligand based drug design  
493 strategies in the development of novel 5-LOX inhibitors. *Current medicinal chemistry*  
494 **2012**, *19*, 3763–3778.
- 495 (15) Sliwoski, G.; Kothiwale, S.; Meiler, J.; Lowe, E. W. Computational methods in drug  
496 discovery. *Pharmacological reviews* **2014**, *66*, 334–395.
- 497 (16) Zhang, W.; Pei, J.; Lai, L. Computational multitarget drug design. *Journal of chemical*  
498 *information and modeling* **2017**, *57*, 403–412.
- 499 (17) Wu, S.; Skolnick, J.; Zhang, Y. Ab initio modeling of small proteins by iterative  
500 TASSER simulations. *BMC biology* **2007**, *5*, 17.
- 501 (18) Lee, J.; Freddolino, P. L.; Zhang, Y. *From protein structure to function with bioinfor-*  
502 *matics*; Springer, 2017; pp 3–35.
- 503 (19) Roy, A.; Kucukural, A.; Zhang, Y. I-TASSER: a unified platform for automated protein  
504 structure and function prediction. *Nature protocols* **2010**, *5*, 725.

- 505 (20) Ferreira, L. G.; dos Santos, R. N.; Oliva, G.; Andricopulo, A. D. Molecular docking and  
506 structure-based drug design strategies. *Molecules* **2015**, *20*, 13384–13421.
- 507 (21) Mandal, S.; Moudgil, M.; Mandal, S. K. Rational drug design. *European journal of*  
508 *pharmacology* **2009**, *625*, 90–100.
- 509 (22) Hamza, A.; Wei, N.-N.; Zhan, C.-G. Ligand-based virtual screening approach using a  
510 new scoring function. *Journal of chemical information and modeling* **2012**, *52*, 963–974.
- 511 (23) Yang, S.-Y. Pharmacophore modeling and applications in drug discovery: challenges  
512 and recent advances. *Drug discovery today* **2010**, *15*, 444–450.
- 513 (24) Ginn, C. M.; Willett, P.; Bradshaw, J. *Virtual Screening: An Alternative or Comple-*  
514 *ment to High Throughput Screening?*; Springer, 2000; pp 1–16.
- 515 (25) Willett, P. Similarity-based virtual screening using 2D fingerprints. *Drug discovery to-*  
516 *day* **2006**, *11*, 1046–1053.
- 517 (26) Willett, P. Combination of similarity rankings using data fusion. *Journal of chemical*  
518 *information and modeling* **2013**, *53*, 1–10.
- 519 (27) Xie, L.; Xie, L.; Bourne, P. E. Structure-based systems biology for analyzing off-target  
520 binding. *Current opinion in structural biology* **2011**, *21*, 189–199.
- 521 (28) March-Vila, E.; Pinzi, L.; Sturm, N.; Tinivella, A.; Engkvist, O.; Chen, H.; Rastelli, G.  
522 On the integration of in silico drug design methods for drug repurposing. *Frontiers in*  
523 *pharmacology* **2017**, *8*, 298.
- 524 (29) Tan, L.; Geppert, H.; Sisay, M. T.; Gütschow, M.; Bajorath, J. Integrating Structure-  
525 and Ligand-Based Virtual Screening: Comparison of Individual, Parallel, and Fused  
526 Molecular Docking and Similarity Search Calculations on Multiple Targets. *ChemMed-*  
527 *Chem* **2008**, *3*, 1566–1571.



- 528 (30) Berenger, F.; Vu, O.; Meiler, J. Consensus queries in ligand-based virtual screening  
529 experiments. *Journal of Cheminformatics* **2017**, *9*, 60.
- 530 (31) Lamb, J.; Crawford, E. D.; Peck, D.; Modell, J. W.; Blat, I. C.; Wrobel, M. J.; Lerner, J.;  
531 Brunet, J.-P.; Subramanian, A. et al. The Connectivity Map: using gene-expression  
532 signatures to connect small molecules, genes, and disease. *science* **2006**, *313*, 1929–  
533 1935.
- 534 (32) Peyvandipour, A.; Saberian, N.; Shafi, A.; Donato, M.; Draghici, S. A novel computa-  
535 tional approach for drug repurposing using systems biology. *Bioinformatics* **2018**, *1*,  
536 9.
- 537 (33) Sawada, R.; Iwata, H.; Mizutani, S.; Yamanishi, Y. Target-based drug repositioning  
538 using large-scale chemical–protein interactome data. *Journal of chemical information*  
539 *and modeling* **2015**, *55*, 2717–2730.
- 540 (34) Lavecchia, A. Machine-learning approaches in drug discovery: methods and applica-  
541 tions. *Drug discovery today* **2015**, *20*, 318–331.
- 542 (35) Aliper, A.; Plis, S.; Artemov, A.; Ulloa, A.; Mamoshina, P.; Zhavoronkov, A. Deep  
543 learning applications for predicting pharmacological properties of drugs and drug re-  
544 purposing using transcriptomic data. *Molecular pharmaceutics* **2016**, *13*, 2524–2530.
- 545 (36) Preuer, K.; Lewis, R. P.; Hochreiter, S.; Bender, A.; Bulusu, K. C.; Klambauer, G.  
546 DeepSynergy: Predicting anti-cancer drug synergy with Deep Learning. *Bioinformatics*  
547 **2017**, *1*, 9.
- 548 (37) Yella, J.; Yaddanapudi, S.; Wang, Y.; Jegga, A. Changing trends in computational drug  
549 repositioning. *Pharmaceutics* **2018**, *11*, 57.
- 550 (38) Yang, H.-T.; Ju, J.-H.; Wong, Y.-T.; Shmulevich, I.; Chiang, J.-H. Literature-based

- 551 discovery of new candidates for drug repurposing. *Briefings in bioinformatics* **2017**,  
552 *18*, 488–497.
- 553 (39) Deftereos, S. N.; Andronis, C.; Friedla, E. J.; Persidis, A.; Persidis, A. Drug repur-  
554 posing and adverse event prediction using high-throughput literature analysis. *Wiley*  
555 *Interdisciplinary Reviews: Systems Biology and Medicine* **2011**, *3*, 323–334.
- 556 (40) Xu, H.; Aldrich, M. C.; Chen, Q.; Liu, H.; Peterson, N. B.; Dai, Q.; Levy, M.; Shah, A.;  
557 Han, X. et al. Validating drug repurposing signals using electronic health records: a case  
558 study of metformin associated with reduced cancer mortality. *Journal of the American*  
559 *Medical Informatics Association* **2014**, *22*, 179–191.
- 560 (41) Zhu, C.; Wu, C.; Jegga, A. G. Network biology methods for drug repositioning. *Post*  
561 *Genom. Approaches Drug Vaccine Dev* **2015**, *5*, 115.
- 562 (42) Green, J. R.; Lotfi Shahreza, M.; Ghadiri, N.; Mousavi, S. R.; Varshosaz, J. A review  
563 of network-based approaches to drug repositioning. *Briefings in Bioinformatics* **2017**,  
564 *19*, 878–892.
- 565 (43) Johnson, M. A.; Maggiora, G. M. *Concepts and applications of molecular similarity*;  
566 Wiley, 1990.
- 567 (44) Maggiora, G.; Vogt, M.; Stumpfe, D.; Bajorath, J. Molecular similarity in medicinal  
568 chemistry: miniperspective. *Journal of medicinal chemistry* **2013**, *57*, 3186–3204.
- 569 (45) Minie, M.; Chopra, G.; Sethi, G.; Horst, J.; White, G.; Roy, A.; Hatti, K.; Samudrala, R.  
570 CANDO and the infinite drug discovery frontier. *Drug discovery today* **2014**, *19*, 1353–  
571 1363.
- 572 (46) Sethi, G.; Chopra, G.; Samudrala, R. Multiscale modelling of relationships between  
573 protein classes and drug behavior across all diseases using the CANDO platform. *Mini*  
574 *reviews in medicinal chemistry* **2015**, *15*, 705–717.

- 575 (47) Chopra, G.; Samudrala, R. Exploring polypharmacology in drug discovery and repur-  
576 posing using the CANDO platform. *Current pharmaceutical design* **2016**, *22*, 3109–  
577 3123.
- 578 (48) Fine, J.; Lackner, R.; Samudrala, R.; Chopra, G. Computational Chemoproteomics to  
579 Understand the Role of Selected Psychoactives in Treating Mental Health Indications.  
580 *ChemRxiv* **2018**,
- 581 (49) Jenwitheesuk, E.; Samudrala, R. Identification of potential multitarget antimalarial  
582 drugs. *JAMA* **2005**, *294*, 1487–1491.
- 583 (50) Jenwitheesuk, E.; Horst, J. A.; Rivas, K. L.; Van Voorhis, W. C.; Samudrala, R. Novel  
584 paradigms for drug discovery: computational multitarget screening. *Trends in pharma-  
585 cological sciences* **2008**, *29*, 62–71.
- 586 (51) Horst, J. A.; Laurenzi, A.; Bernard, B.; Samudrala, R. Computational multitarget drug  
587 discovery. *Polypharmacology in Drug Discovery* **2012**, 263–301.
- 588 (52) Medina-Franco, J. L.; Giulianotti, M. A.; Welmaker, G. S.; Houghten, R. A. Shifting  
589 from the single to the multitarget paradigm in drug discovery. *Drug discovery today*  
590 **2013**, *18*, 495–501.
- 591 (53) Boran, A. D.; Iyengar, R. Systems approaches to polypharmacology and drug discovery.  
592 *Current opinion in drug discovery & development* **2010**, *13*, 297.
- 593 (54) Reddy, A. S.; Zhang, S. Polypharmacology: drug discovery for the future. *Expert review  
594 of clinical pharmacology* **2013**, *6*, 41–47.
- 595 (55) Anighoro, A.; Bajorath, J.; Rastelli, G. Polypharmacology: challenges and opportu-  
596 nities in drug discovery: miniperspective. *Journal of medicinal chemistry* **2014**, *57*,  
597 7874–7887.

- 598 (56) Iwata, M.; Hirose, L.; Kohara, H.; Liao, J.; Sawada, R.; Akiyoshi, S.; Tani, K.; Yaman-  
599 ishi, Y. Pathway-Based Drug Repositioning for Cancers: Computational Prediction and  
600 Experimental Validation. *Journal of medicinal chemistry* **2018**, *61*, 9583–9595.
- 601 (57) Todeschini, R.; Consonni, V.; Xiang, H.; Holliday, J.; Buscema, M.; Willett, P. Similar-  
602 ity coefficients for binary chemoinformatics data: overview and extended comparison  
603 using simulated and real data sets. *Journal of chemical information and modeling* **2012**,  
604 *52*, 2884–2901.
- 605 (58) Tanimoto, T. T. IBM internal report. *Nov* **1957**, *17*, 1957.
- 606 (59) Hert, J.; Keiser, M. J.; Irwin, J. J.; Oprea, T. I.; Shoichet, B. K. Quantifying the  
607 relationships among drug classes. *Journal of chemical information and modeling* **2008**,  
608 *48*, 755–765.
- 609 (60) Bajusz, D.; Rácz, A.; Héberger, K. Why is Tanimoto index an appropriate choice for  
610 fingerprint-based similarity calculations? *Journal of cheminformatics* **2015**, *7*, 20.
- 611 (61) Landrum, G. RDKit: Open-source cheminformatics. 2006; [rdkit.org](http://rdkit.org).
- 612 (62) Cereto-Massagué, A.; Ojeda, M. J.; Valls, C.; Mulero, M.; Garcia-Vallvé, S.; Pujadas, G.  
613 Molecular fingerprint similarity search in virtual screening. *Methods* **2015**, *71*, 58–63.
- 614 (63) Mangione, W.; Samudrala, R. Identifying Protein Features Responsible for Improved  
615 Drug Repurposing Accuracies Using the CANDO Platform: Implications for Drug De-  
616 sign. *Molecules* **2019**, *24*.
- 617 (64) Bolton, E. E.; Wang, Y.; Thiessen, P. A.; Bryant, S. H. *Annual reports in computational*  
618 *chemistry*; Elsevier, 2008; Vol. 4; pp 217–241.
- 619 (65) Berman, H. M.; Westbrook, J.; Feng, Z.; Gilliland, G.; Bhat, T. N.; Weissig, H.;  
620 Shindyalov, I. N.; Bourne, P. E. *International Tables for Crystallography Volume F:*  
621 *Crystallography of biological macromolecules*; Springer, 2006; pp 675–684.

- 622 (66) Davis, A. P.; Grondin, C. J.; Johnson, R. J.; Sciaky, D.; King, B. L.; McMorran, R.;  
623 Wieggers, J.; Wieggers, T. C.; Mattingly, C. J. The comparative toxicogenomics database:  
624 update 2017. *Nucleic acids research* **2016**, *45*, D972–D978.
- 625 (67) Rogers, D.; Hahn, M. Extended-connectivity fingerprints. *Journal of chemical informa-*  
626 *tion and modeling* **2010**, *50*, 742–754.
- 627 (68) Hassan, M.; Brown, R. D.; Varma-O’Brien, S.; Rogers, D. Cheminformatics analysis  
628 and learning in a data pipelining environment. *Molecular diversity* **2006**, *10*, 283–299.
- 629 (69) Arany, A.; Bolgár, B.; Balogh, B.; Antal, P.; Mátyus, P. Multi-aspect candidates for  
630 repositioning: data fusion methods using heterogeneous information sources. *Current*  
631 *medicinal chemistry* **2013**, *20*, 95–107.
- 632 (70) others,, et al. Colistin as a potentiator of anti-TB drug activity against *Mycobacterium*  
633 *tuberculosis*. *The Journal of antimicrobial chemotherapy* **2015**, *70*, 2828–2837.
- 634 (71) Apoorv, T. S.; Babu, P. P. Minocycline prevents cerebral malaria, confers neuroprotec-  
635 tion and increases survivability of mice during *Plasmodium berghei* ANKA infection.  
636 *Cytokine* **2017**, *90*, 113–123.
- 637 (72) Centers for Disease Control and Prevention Yellow Book 2018: Health Information for  
638 International Travel. **2017**,
- 639 (73) Sahu, R.; Walker, L. A.; Tekwani, B. L. In vitro and in vivo anti-malarial activity of  
640 tigecycline, a glycylicycline antibiotic, in combination with chloroquine. *Malaria journal*  
641 **2014**, *13*, 414.
- 642 (74) Starzengruber, P.; Thriemer, K.; Haque, R.; Khan, W.; Fuehrer, H.; Siedl, A.;  
643 Hofecker, V.; Ley, B.; Wernsdorfer, W. et al. Antimalarial activity of tigecycline, a  
644 novel glycylicycline antibiotic. *Antimicrobial agents and chemotherapy* **2009**, *53*, 4040–  
645 4042.

- 646 (75) Perronne, C. Antiviral hepatitis and antiretroviral drug interactions. *Journal of hepato-*  
647 *tology* **2006**, *44*, S119.
- 648 (76) Cummings, J. L.; Lyketsos, C. G.; Peskind, E. R.; Porsteinsson, A. P.; Mintzer, J. E.;  
649 Scharre, D. W.; Jose, E.; Agronin, M.; Davis, C. S. et al. Effect of dextromethorphan-  
650 quinidine on agitation in patients with Alzheimer disease dementia: a randomized  
651 clinical trial. *Jama* **2015**, *314*, 1242–1254.
- 652 (77) Costin, J. M.; Jenwitheesuk, E.; Lok, S.-M.; Hunsperger, E.; Conrads, K. A.;  
653 Fontaine, K. A.; Rees, C. R.; Rossmann, M. G.; Isern, S. et al. Structural optimization  
654 and de novo design of dengue virus entry inhibitory peptides. *PLoS neglected tropical*  
655 *diseases* **2010**, *4*, e721.
- 656 (78) Nicholson, C. O.; Costin, J. M.; Rowe, D. K.; Lin, L.; Jenwitheesuk, E.; Samudrala, R.;  
657 Isern, S.; Michael, S. F. Viral entry inhibitors block dengue antibody-dependent en-  
658 hancement in vitro. *Antiviral research* **2011**, *89*, 71–74.
- 659 (79) Michael, S.; Isern, S.; Garry, R.; Samudrala, R.; Costin, J.; Jenwitheesuk, E. Optimized  
660 dengue virus entry inhibitory peptide (dn81). 2012.
- 661 (80) Michael, S.; Isern, S.; Costin, J.; Samudrala, R.; Jenwitheesuk, E. Optimized dengue  
662 virus entry inhibitory peptide (10an). 2014.
- 663 (81) Hughes, J. P.; Rees, S.; Kalindjian, S. B.; Philpott, K. L. Principles of early drug  
664 discovery. *British journal of pharmacology* **2011**, *162*, 1239–1249.
- 665 (82) Falls, Z.; Mangione, W.; Schuler, J.; Samudrala, R. Exploration of interaction scoring  
666 criteria in the CANDOR platform. *To appear* **2019**,
- 667 (83) Hudson, M.; Samudrala, R. Optimized Virtual Screening for Drug Repurposing Oppor-  
668 tunities. **2019**, To appear.

- 669 (84) Fine, J. A.; Konc, J.; Samudrala, R.; Chopra, G. CANDOCK: Chemical atomic network  
670 based hierarchical flexible docking algorithm using generalized statistical potentials.  
671 *bioRxiv* **2018**, 442897.
- 672 (85) Fine, J. A.; Chopra, G. CANDOCK: Conformational Entropy Driven Analytics for  
673 Class-Specific Proteome-Wide Docking. *Biophysical Journal* **2018**, *114*, 57a.
- 674 (86) Trott, O.; Olson, A. J. AutoDock Vina: improving the speed and accuracy of docking  
675 with a new scoring function, efficient optimization, and multithreading. *Journal of*  
676 *computational chemistry* **2010**, *31*, 455–461.
- 677 (87) Garattini, S. Are me-too drugs justified? *Journal of Nephrology* **1997**, *10*, 283–294.
- 678 (88) Régnier, S. What is the value of ‘me-too’ drugs? *Health care management science* **2013**,  
679 *16*, 300–313.
- 680 (89) O’Boyle, N. M.; Sayle, R. A. Comparing structural fingerprints using a literature-based  
681 similarity benchmark. *Journal of cheminformatics* **2016**, *8*, 36.
- 682 (90) Sastry, M.; Lowrie, J. F.; Dixon, S. L.; Sherman, W. Large-scale systematic analysis  
683 of 2D fingerprint methods and parameters to improve virtual screening enrichments.  
684 *Journal of chemical information and modeling* **2010**, *50*, 771–784.
- 685 (91) Zuma, A. A.; Cavalcanti, D. P.; Zogovich, M.; Machado, A. C. L.; Mendes, I. C.;  
686 Thiry, M.; Galina, A.; de Souza, W.; Machado, C. R. et al. Unveiling the effects of  
687 berenil, a DNA-binding drug, on *Trypanosoma cruzi*: implications for kDNA ultra-  
688 structure and replication. *Parasitology Research* **2015**, *114*, 419–430.
- 689 (92) Melnikov, S. V.; Söll, D.; Steitz, T. A.; Polikanov, Y. S. Insights into RNA binding by  
690 the anticancer drug cisplatin from the crystal structure of cisplatin-modified ribosome.  
691 *Nucleic Acids Research* **2016**, *44*, 4978–4987.

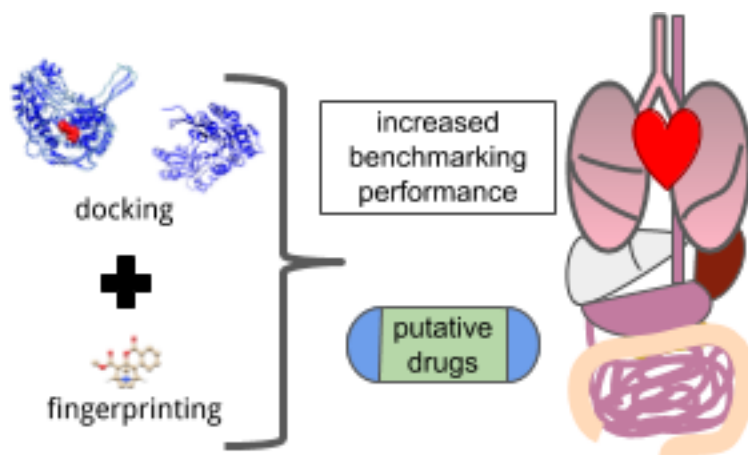


Figure 4: For Table of Contents Only